JOC Article

Tautomerization of 2-Acetylcyclohexanone. 1. Characterization of Keto−Enol/Enolate Equilibria and Reaction Rates in Water

Emilia Iglesias

Dpto de Química Física e E. Q. I. Facultad de Ciencias, Universidad de La Coruña, 15071-La Coruña, Spain

qfemilia@udc.es

Received October 30, 2002

The keto−enol tautomerism of 2-acetylcyclohexanone (ACHE) was studied in water under different experimental conditions. By contrast with other previously studied β-diketones, the keto−enol interconversion in the ACHE system is a slow process. Under equilibrium conditions, the analysis of the absorbance readings of ACHE aqueous solutions yielded more than 40% of enol content at 25 °C; nevertheless, in aprotic solvents such as dioxane, ACHE is almost completely enolized. In alkaline medium, the enolate ion is the only existing species; the study of the effect of pH on the UV-absorption spectrum of ACHE yielded a value of 9.85 for the overall pK_a of ACHE. Under nonequilibrium conditions, the keto−enol tautomerization was studied in water. Several factors affecting the reaction have been investigated, which include H^+-catalysis, ionic strength effect, buffer catalysis, deuterium isotope effects, temperature effect, or solvent effects.

Introduction

Enols and enolate ions are critical intermediates in many important reactions. The work of Lapworth on the acid-catalyzed halogenation of acetone suggested, for the first time, the formation of acetone−enol in the rate-determining step which precedes involvement of halogen.[1] Since that time, several thousand papers have made enolization a well-documented process.[2−6]

Early estimations of the enol content of simple carbonyl compounds used the heat of formation of the related methyl ether or the entropy terms and the Gibbs free energy differences between enols and ethers to evaluate enol formation equilibrium constants.[7] Other methods estimated the ketonization rate constants as being equal to the rate constants for hydrolysis of the corresponding methyl enol ethers. The equilibrium constants were then calculated as the ratios between H^+-catalyzed enolization and H^+-catalyzed hydrolysis rate constants.[8] Usually these independent methods have led to a much lower enol content than that obtained by the halogen titration method, which becomes very difficult to apply when the enol content is very low, leading to ambiguous results; in addition, the halogenation rate constant is assumed as the value of a diffusion-controlled process.[9]

The generally very low enol content of simple ketones had, for a long time, restricted studies of keto−enol interconversion to examination of only the enolization reaction. In the past few years, Kresge et al.[10−15] have developed new methods to carry out an extensive and very precise work on keto−enol interconversion of "simple" enols of β-ketoacids, α-ketoesters, or β-ketoamides.

In contrast to the low enol content of monocarbonyl compounds, the enol form of the tautomeric species of 1,3-diketones sometimes predominates over the corresponding keto form. Solvent effects on the equilibrium position of these compounds are pronounced, due to the enol form is stabilized by intramolecular O−H···O hydrogen bonds. This fact facilitates the study of their keto−enol interconversion, and there have been extensive studies of the reaction in water as well as in organic solvents.[16−19]

During the past few years, the keto−enol interconver-

(1) Lapworth, A. *J. Chem. Soc.* **1904**, 30.
(2) Forsén, S.; Nilson, M. In *The Chemistry of the Carbonyl Group*; Zabicky, J., Ed.; Interscience: London, 1970; pp 157−240.
(3) Hart, H. *Chem. Rev.* **1979**, *79*, 515.
(4) Toullec, J. *Adv. Phys. Org. Chem.* **1982**, *18*, 1.
(5) Rappoport, Z.; Biali, S. E. *Acc. Chem. Res.* **1988**, *21*, 442.
(6) *The Chemistry of the Enols*; Rappoport, Z., Ed.; Wiley: Chichester, England, 1990.
(7) Guthrie, J. P. In *The Chemistry of the Enols*; Rappoport, Z., Ed.; Wiley: Chichester, England, 1990; pp 75−93.
(8) Guthrie, J. P. *Can. J. Chem.* **1979**, *57*, 236; **1979**, *57*, 797; **1979**, *57*, 1177.
(9) Gero, A. *J. Org. Chem.* (a) **1954**, *19*, 469; (b) **1954**, *19*, 1960; (c) **1961**, *26*, 3156.
(10) Kresge, A. J. *Chem. Soc. Rev.* **1996**, 275.
(11) Kresge, A. J. *Acc. Chem. Res.* **1990**, *23*, 43.
(12) Kresge, A. J. In *The Chemistry of the Enols*; Rappoport, Z., Ed.; Wiley: Chichester, England, 1990; pp 399−480.
(13) Chiang, Y.; Gue, H.-X.; Kresge, A. J.; Tee, O. S. *J. Am. Chem. Soc.* **1996**, *118*, 3386. Chiang, Y.; Kresge, A. J.; Nikolaev, V. A.; Popik, V. V. *J. Am. Chem. Soc.* **1997**, *119*, 11183. Chiang, Y.; Kresge, A. J.; Meng, Q.; Morita, Y.; Yamamoto, Y. *J. Am. Chem. Soc.* **1999**, *121*, 8345.
(14) Chiang, Y.; Kresge, A. J.; Schepp, N. P.; Xie, R.-Q. *J. Org. Chem.* **2000**, *65*, 1175.
(15) Chiang, Y.; Criesbeck, A. G.; Heckroth, H.; Hellrung, B.; Kresge, A. J.; Meng, Q.; O'Donoghue, A. C.; Richard, J. P.; Wirz, J. *J. Am. Chem. Soc.* **2001**, *123*, 8979.
(16) Morton, R. A.; Hassan, T.; Calloway, T. C. *J. Chem. Soc.* **1934**, 883.
(17) Murthy, A. S. N.; Balasubramanian, A.; Rao, C. N. R.; Kasturi, T. R. *Can. J. Chem.* **1962**, *40*, 2267.
(18) Mills, S. G.; Beak, P. *J. Org. Chem.* **1985**, *50*, 1216.
(19) Toullec, J. *The Chemistry of the Enols*; Rappoport, Z., Ed.; Wiley: Chichester, England, 1990; pp 323−398.

10.1021/jo026629x CCC: $25.00
Published on Web 02/21/2003

SCHEME 1. Structures of 1,3-Dicarbonyl Compounds That Show Rapid Keto−Enol Tautomerization

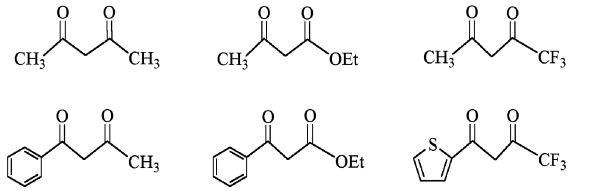

sion of 1,3-diketones or 1,3-ketoesters, as well as their reactivity, was investigated in aqueous solutions of surfactant-forming micelles.[20−27] The research reported in the current work upon the isomerization of 2-acetylcyclohexanone (ACHE) shows that, conversely to the compounds previously studied by us (Scheme 1), or even to its homologous compound, 2-acetylcyclopentanone,[28] *the keto−enol interconversion of ACHE is a slow reaction*. Therefore, we were able to perform a detailed kinetic study of the keto−enol tautomerization of this compound by analyzing several parameters, including salts effects, acid−base catalysis, isotope effects, or the influence of temperature.

Experimental Section

Materials. 2-Acetylcyclohexanone, of the maximum purity, was used as supplied. D_2O was >99.9% isotope enrichment and $d = 1.11$. All other reagents were also used as received. For the buffer plots for the determination of rate constants, the buffers sodium acetate/acetic acid and its chloro- and dichloro-derivatives were used. For determination of the pK_a in the basic pH range, use was made of hydrogen carbonate/carbonate and phosphoric acid(1)/hydrogen phosphate buffers. Aqueous solutions were prepared with doubly distilled water obtained from a permanganate solution. Freshly prepared solutions were used in all experiments.

Methods. UV−vis absorption spectra and kinetic measurements were recorded with a double-beam spectrophotometer provided with a thermostated cell holder. A matched pair of quartz cells with $l = 1$ cm light path was used, especially in obtaining the spectra. The pH was measured with a pH meter equipped with a GK2401B combined glass electrode. The glass electrode was standardized by using commercial standard pH 4.01, 7.01, and 9.26 buffers.

Kinetic measurements were carried out under pseudo-first-order conditions, with the concentration of ACHE, the limiting reagent, being more than 20 times lower than that of the others reactants. The rate of the transformation of the enol form of ACHE to the equilibrium mixture has been studied in water by monitoring the decreasing absorbance at $\lambda = 291$ nm due to the enol form. For that, ACHE was dissolved in dioxane to give a stock solution 0.018 M. The reaction was initiated by injecting 10 μL of this solution into 3.0 mL of water containing the rest of the reagents. Alternatively, ACHE can be dissolved in alkaline medium to yield the enolate quantitatively, which, after acidification, gives the enol with 100% yield. The enol so recovered tautomerizes slowly to the keto form until to achieve the equilibrium proportions.The integrated method was followed throughout, fitting the experimental data (absorbance−time, $A-t$) to eq 1, where A_0, A_∞, and A mean absorbance readings at times 0, infinity, and t, respectively, and k_o represents the pseudo-first-order rate constant. In every case, satisfactory correlation coefficients (r > 0.9999) and residuals were obtained. Under these experimental conditions, a decrease in absorbance ($A_0 - A_\infty$ in eq 1 is positive) at 291 nm from approximately 1 to 0.4 absorbance units was observed.

$$A = A_\infty + (A_0 - A_\infty)e^{-k_o t} \text{ with } k_o = k_o^{\,k} + k_o^{\,e} \qquad (1)$$

As the observed process is an approach to the equilibrium, k_o is the sum of the rate constants corresponding to ketonization (k_o^k) and enolization (k_o^e). For each kinetic run, the pseudo-first-order rate constant for ketonization was then determined as $k_o^k = k_o(A_0 - A_\infty)/A_0$[29] and $k_o^e = k_o - k_o^k$. (Of course, $k_o^k = k_o/(1 + K_E)$, but we used the former expression in order to determine also K_E).

Results

Keto−Enol/Enolate Equilibria. In aprotic solvents, such as dioxane, the enolic form of ACHE is the majority species, whereas in water, a mixture of both the keto and enol tautomers exists. However, contrary to the case of other previously studied 1,3-dicarbonyl compounds, *the keto−enol interconversion in the ACHE system is slow* enough to follow it by conventional methods. In this sense, the recorded spectrum just after the addition of an aliquot of a dioxane solution of ACHE into a sample of water (dilution factor higher than 250) shows an absorption band due to the enol ($\lambda_{max} = 291$ nm) which decreases slowly with time because of the enol conversion into the keto form. Conversely, when an aqueous equilibrated ACHE solution is diluted (∼1:29) in dioxane the absorption band centered at 291 nm increases slowly with time, as a consequence of the conversion of the keto tautomer into the enol. The presence of a well-defined isosbestic point at $\lambda \sim 228$ nm states for the keto−enol equilibrium. Figure 1 shows these experimental observations.

The keto−enol equilibrium constant, K_E, was measured in water from the Beer−Lambert law under nonequilibrium conditions. The substrate ACHE was added to the reaction mixture from a stock dioxane solution, and the rate of approach to equilibrium was observed as a function of ACHE concentration. As ACHE exists in dioxane, mainly as the enol tautomer, the extrapolated absorbance readings at $t \rightarrow 0$ (determined from the fit of $A-t$ to eq 1) correspond to the absorption of the enol, then eq 2 applies. The plot of A^0_{291} against $[ACHE]_t$ yields a good straight line passing through the origin. The slope of this line equals the molar absorption coefficient of the enol at 291 nm, i.e., $\epsilon_{EH} = 15\,270 \pm 200$ mol^{-1} dm^3 cm^{-1} ($r = 0.999_8$). Morton et al.[16] concluded that a given tautomer of 1,3-diketone is substantially independent of the solvent in regard to the spectral location and the molar absorption coefficient of the maxima, which in aprotic solvents reaches values close to 15 000 mol^{-1} dm^3 cm^{-1}, in good agreement with the value determined here. On the other hand, the absorbance readings at $t \rightarrow \infty$

(20) Iglesias, E. *J. Phys. Chem.* **1996**, *100*, 12592.
(21) Iglesias, E. *J. Chem. Soc., Perkin Trans. 2* **1997**, 431.
(22) Iglesias, E. *Langmuir* **2000**, *16*, 8438.
(23) Iglesias, E. *Langmuir* **1998**, *14*, 5764.
(24) Iglesias, E.; Domínguez, A. *New J. Chem.* **1999**, *23*, 851.
(25) Iglesias, E. *Langmuir* **2001**, *17*, 6871.
(26) Iglesias, E. *J. Org. Chem.* **2000**, *65*, 6583.
(27) Iglesias, E. *J. Phys. Chem. B* **2001a**, *105*, 10287; **2001b**, *105*, 10295.
(28) Iglesias, E. *New J. Chem.* **2002**, *26*, 1352.

(29) See for example Laidler, K. J. *Chemical Kinetics*, 3rd ed.; Harper Collins Publishers: New York, 1987; Chapter 2.

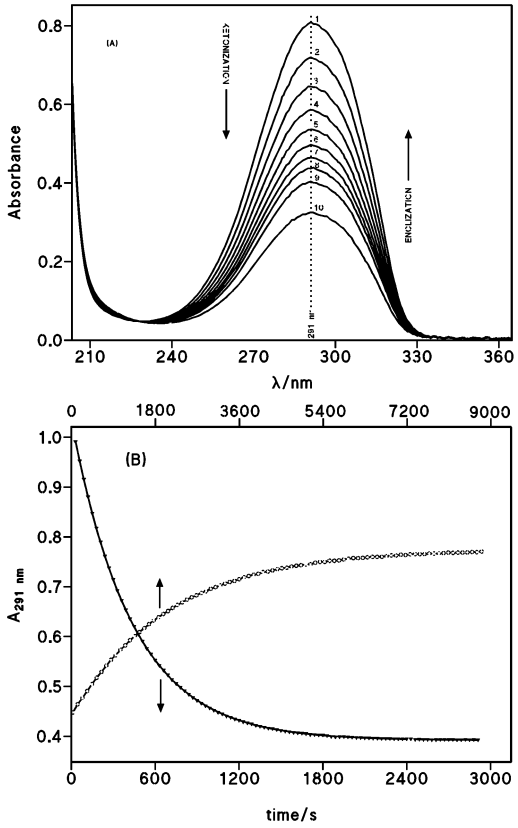

FIGURE 1. (A) Repeat scans (1−8) every 2 min (9 at 3 min, 10 at infinite time) showing the decreasing absorbance due to ketonization of ACHE-enol, [ACHE] = 6.0×10^{-5} M; $[H^+]$ = 0.050 M. (B) Variation of the absorbance at 291 nm as a function of time for (△) enol−ketonization in water, [ACHE] = 6.5×10^{-5} M, $[H^+] = 0.015$ M, and for (○) keto−enolization in 70% v/v dioxane/water, [ACHE] = 6.0×10^{-5} M, $[H^+]$ = 0.013 M. The temperature was 25 °C.

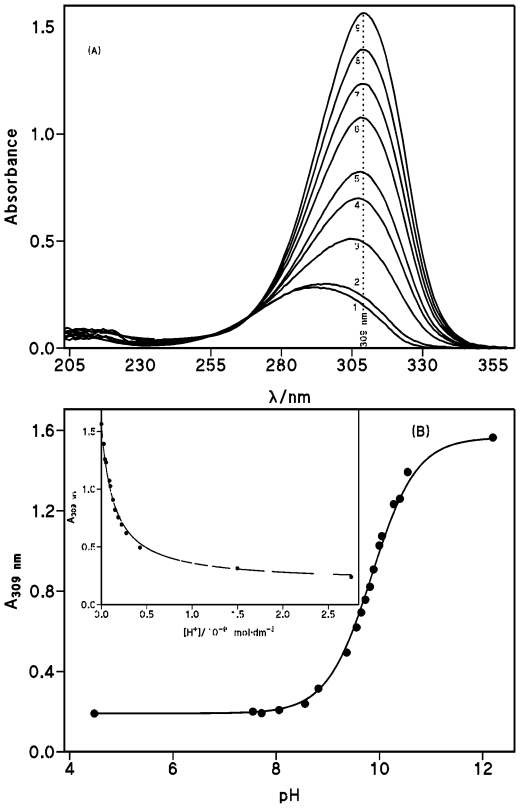

FIGURE 2. (A) Absorption spectrum of ACHE (5.0×10^{-5} M) obtained in water as a function of pH: 1, 7.55; 2, 8.56; 3, 9.37; 4, 9.65; 5, 9.82; 6, 10.05; 7, 10.28; 8, 10.55; 9, [NaOH] = 0.16 M. (B) Spectrophotometric titration curve for the acid ionization of ACHE (5.0×10^{-5} M) in aqueous solutions of the buffers $HPO_4^{2-}/H_2PO_4^-$ and HCO_3^-/CO_3^{2-} at 25 °C. The inset shows the fit of the data A_{309}−$[H^+]$ according to eq 6.

SCHEME 2. Keto−Enol/Enolate Equilibria of ACHE in Aqueous Basic Medium

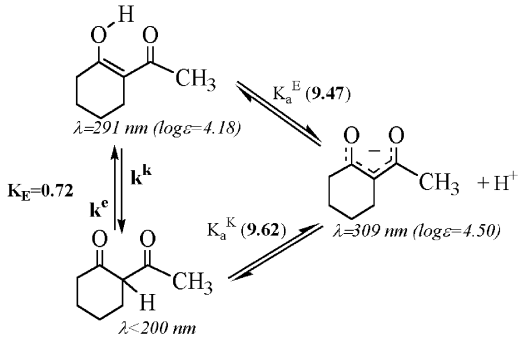

(determined also from the nonlinear regression analysis of $A-t$ data to eq 1) correspond to the absorption of the enol in an equilibrated solution of ACHE, in which case eq 3 applies. The plot of A^{∞}_{291} versus $[ACHE]_t$ results also in a good straight line with a slope value of 6472 ± 100 mol^{-1} dm^3 cm^{-1} (r = 0.9999). The combination of both slope values gives K_E = 0.72, which means more than 40% of enol content of ACHE in water.

$$A^{0}_{291} = \epsilon_{EH} l [ACHE]_t \qquad (2)$$

$$A^{\infty}_{291} = \epsilon_{EH} l \frac{K_E}{1 + K_E} [ACHE]_t \qquad (3)$$

The acid ionization equilibrium constant, K_a, of ACHE was determined from the analysis of its absorption spectrum as a function of pH, which is shown in Figure 2A. This graph is typical of the spectral observations for enolate formation and implies a clean equilibration of the acidic species (the keto and enol tautomers) with their common conjugate base, the enolate (Scheme 2).

Enolate anions are ambident species and the equilibrium enolization constant, K_E, linking the two tautomeric protonated forms, is a function of the acidity constants of these two species. Thus, titration of an equilibrium mixture of keto (KH) and enol (EH) tautomers yields a mixed acid ionization constant, K_a, whose value corresponds to the pH of the inflection point. This acid ionization constant measured in water can be defined as in eq 4.

$$\frac{1}{K_a} = \frac{[EH] + [KH]}{[E^-]_t [H^+]} = \frac{1}{K_a^E} + \frac{1}{K_a^K} \qquad (4)$$

The absorbance readings at the maximum wavelength (λ = 309 nm) describe a sigmoid curve on varying the pH, Figure 2B. This absorption is due to both the enol and enolate species; then $A_{309} = \epsilon_{EH} l [EH] + \epsilon_E l [E^-]$. By considering the mass balance equation, $[ACHE]_t = [KH]$

TABLE 1. Observed Characteristics for the Three Forms (Keto, Enol, and Enolate) of 2-Acetylcyclohexanone Existing in Water

	keto (KH)	enol (EH)	enolate (E)
λ_{max}/nm	<200	291	309
ϵ/mol^{-1} dm^3 cm^{-1}	-	15270	34200
pK_a^i	9.62	9.47 (9.47)[a]	
K_E	0.72−0.75 (0.41)[a]		
pK_a		9.85 (9.85)[a]	

[a] Values obtained by Riley and Long[30] in the bromination of this ketone.

+ [EH] + [E$^-$] and the expression of K_a, the eq 5 is derived, where A_a and A_b refer to the absorbance readings at very low and very high pH, respectively.

$$A_{309} = \frac{A_a 10^{pK_a} + A_b 10^{pH}}{10^{pK_a} + 10^{pH}} \quad (5)$$

The solid sigmoid curve in Figure 2B was constructed with the experimental values of $A_a = 0.191$ and $A_b = 1.565$ and the adjusted value of p$K_a = 9.85 \pm 0.01$ ($r = 0.999_5$). From the latter value and by making used of K_E determined previously, the relationships of $K_a = K_a^K/(1 + K_E)$ or $K_a = K_a^E K_E/(1 + K_E)$, give p$K_a^K = 9.62$ and p$K_a^E = 9.47$, respectively to the pK_a values of the keto and enol tautomers. These results show that the stronger acid (enol) of a pair of compounds in equilibrium with a common anion (enolate) is the minor component of the mixture. Alternatively, the experimental data of $A_{309}-$[H$^+$] may be related through eq 6, where A_{EH}^∞ and A_E^∞ correspond to the absorbance readings when all the [ACHE] is in the enol or enolate forms, respectively. The solid line in the inset of Figure 2B fits eq 6 to the experimental points when $K_a^E = (3.2 \pm 0.1)10^{-10}$ mol dm^{-3}; $(1 + K_E)/K_E = 2.55 \pm 0.08$; $A_{EH}^\infty = 0.45 \pm 0.03$, and $A_E^\infty = 1.608 \pm 0.020$. These results imply p$K_a^E = 9.49$; $K_E = 0.65$, and $\epsilon_E = 32\ 160$ mol^{-1} dm^3 cm^{-1}, in good agreement with the expected values. All these results are summarized in Table 1.

$$A_{309} = \frac{A_{EH}^\infty [H^+] + A_E^\infty K_a^E}{K_a^E + \frac{1 + K_E}{K_E}[H^+]} \quad (6)$$

Rates of Keto−Enol Tautomerization. The ketonization reaction of the enol tautomer of ACHE was studied by monitoring the decreasing absorbance at $\lambda =$ 291 nm.

Influence of Ionic Strength. The ionic strength dependence of k_0, the first-order rate constant for reaction of the enol to form the equilibrium mixtures, was analyzed at [H$^+$] = 0.05 M (HCl) by varying NaCl concentration. The results reveal no appreciable effect of this parameter in the range of ionic strength investigated (0.05 to 1 M); for instance, $k_0 = 1.68 \times 10^{-3}$ s^{-1} (or $k_0^k = 1.0 \times 10^{-3}$ s^{-1}) at $I = 0.08$ M; $k_0 = 1.65 \times 10^{-3}$ s^{-1} (or $k_0^k = 0.98 \times 10^{-3}$ s^{-1}) at $I = 0.45$ M, and $k_0 = 1.61 \times 10^{-3}$ s^{-1} (or $k_0^k = 0.98 \times 10^{-3}$ s^{-1}) at $I = 0.95$ M.

Influence of [H$^+$]. Rate constants for ketonization were measured as a function of [H$^+$] (HCl) at 25 °C at 0.20, 0.40, and 0.75 M ionic strength (NaCl). The set of experiments at I = 0.20 M was performed by dissolving

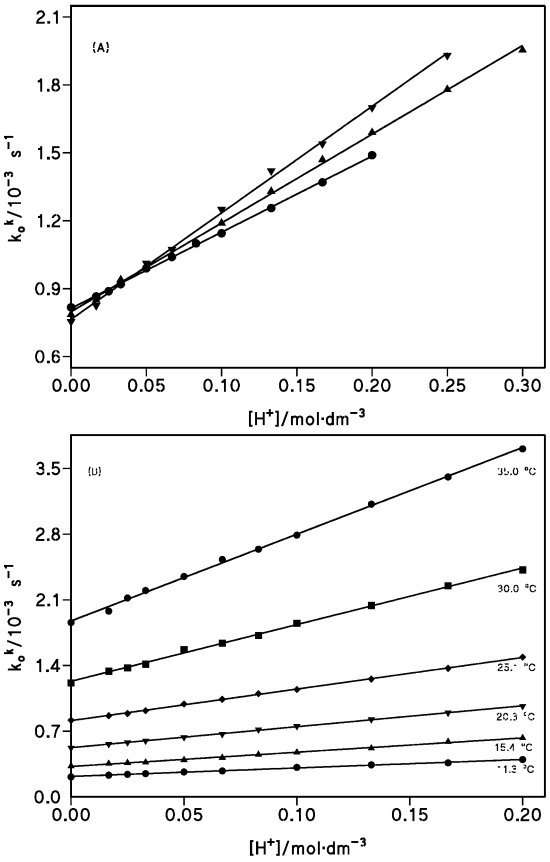

FIGURE 3. Variation of the observed rate constant for ACHE−enol ketonization, k_o^k, as a function of [H$^+$] (A) at 25 °C and ionic strength, controlled with NaCl, (●) 0.20 M, (▲) 0.40 M, and (▼) 0.75 M, and (B) at $I = 0.20$ M and different temperatures.

ACHE in alkaline medium ([NaOH] = 0.017 M); subsequently the reaction mixture was acidified with the required amount of HCl to reach the desired [H$^+$]. The ketonization rates of the enol generated in situ were studied as a function of [H$^+$]. Figure 3A shows the variation of the observed rate constants as a function of [H$^+$], where eq 7 applies. Least-squares fitting of this equation to the experimental data yields the rate constants listed in Table 2.

$$k_0^k = k_w^k + k_H^k[H^+] \quad (7)$$

Isotopic Effects. Rates of ketonization were also measured in dilute D_2O solutions of hydrochloric acid at $I = 0.20$ M (NaCl). The results are reported in Table 2. One can note the lower rate constant observed in D_2O than in H_2O. The combination of the data obtained for ketonization process in these two solvents at the same ionic strength gives large kinetic isotope effects for the uncatalyzed reaction: $k_w^{k(H_2O)}/k_w^{k(D_2O)} = 8.2$ (or $k_w^{e(H_2O)}/k_w^{e(D_2O)} = 9.1$), whereas lower isotope effects for H$^+$-catalyzed reaction was observed: $k_H^k/k_D^k = 3.2$ (or $k_H^e/k_D^e = 3.6$).

Activation Parameters. The influence of [H$^+$] at ionic strength 0.20 M on rates of ketonization of ACHE−enol in water was studied at several temperatures ranging from 283 to 308 K. The obtained k_0^k (or k_0^e) values as a function of both [H$^+$] and temperature are displayed in

TABLE 2. Experimental Conditions and Rate Constants Obtained in the Ketonization of ACHE Performed in H_2O and D_2O at Several Ionic Strengths and Temperatures

I/M	T/°C	$k_w/10^{-3}$ s^{-1}[a]	k_H/mol^{-1} dm^3 s^{-1}[a]	k_w^k/s^{-1}	k_H^k/mol^{-1} dm^3 s^{-1}	K_E[b]
0.20[c]	25	1.393 ± 0.003	(5.84 ± 0.05) × 10^{-3}	8.52 × 10^{-4}	3.87 × 10^{-3}	0.68
0.20	25	1.395 ± 0.004	(5.80 ± 0.02) × 10^{-3}	8.11 × 10^{-4}	3.37 × 10^{-3}	0.72
0.40	25	1.306 ± 0.005	(6.67 ± 0.03) × 10^{-3}	7.68 × 10^{-4}	3.92 × 10^{-3}	0.69
0.75	25	1.215 ± 0.004	(8.14 ± 0.03) × 10^{-3}	7.15 × 10^{-4}	4.79 × 10^{-3}	0.71
0.20[d]	25	1.35 ± 0.01[e]		8.10 × 10^{-4}		
0.10[d]	25	1.377 ± 0.002		8.31 × 10^{-4}		
0.20[f]	**25**	**0.163 ± 0.001**	**(1.72 ± 0.02) × 10^{-3}**	**1.06 × 10^{-4}**	**1.12 × 10^{-3}**	**0.65**
0.20	11.3	0.382 ± 0.0016	(1.466 ± 0.015) × 10^{-3}	2.25 × 10^{-4}	0.86 × 10^{-3}	0.71
0.20	15.4	0.549 ± 0.008	(2.57 ± 0.08) × 10^{-3}	3.23 × 10^{-4}	1.51 × 10^{-3}	0.71
0.20	20.3	0.892 ± 0.003	(3.79 ± 0.03) × 10^{-3}	5.25 × 10^{-4}	2.23 × 10^{-3}	0.69
0.20	25.1	1.393 ± 0.005	(5.84 ± 0.05) × 10^{-3}	8.19 × 10^{-4}	3.44 × 10^{-3}	0.72
0.20	30.0	2.03 ± 0.02	(10.2 ± 0.2) × 10^{-3}	11.9 × 10^{-4}	6.02 × 10^{-3}	0.66
0.20	35.0	3.09 ± 0.01	(15.65 ± 0.1) × 10^{-3}	18.1 × 10^{-4}	9.21 × 10^{-3}	0.66

isotope effects: $k_w^k(H_2O)/k_w^k(D_2O) = 8.2$, $k_H^k/k_D^k = 3.2$; $k_w^e(H_2O)/k_w^e(D_2O) = 9.1$, $k_H^e/k_D^e = 3.6$

[a] $k_o = k_w + k_H[H^+]$. [b] Average value of at least nine determinations. [c] ACHE-enol generated in situ. [d] Reaction in pure water, $k_w = k_w^k + k_w^e$; obtained from the fit of eq 1 to the experimental data $A-t$. [e] Mean value of two determinations. [f] Reaction in D_2O.

TABLE 3. Activated Parameters Corresponding to the Water-Catalyzed Reaction (k_{H2O}) and H^+-Catalyzed Reaction (k_H) for Both the Ketonization and Enolization Reactions of ACHE

	ketonization reaction in water (k_o^k)		enolization reaction in water (k_o^e)	
reaction	$\Delta H^‡$ (kJ/mol)	$\Delta S^‡$ (J/mol·K)	$\Delta H^‡$ (kJ/mol)	$\Delta S^‡$ (J/mol·K)
$k_w/[H_2O]$/mol^{-1} dm^3 s^{-1}	63.8	−140	59.6	−107.4
k_H/mol^{-1} dm^3 s^{-1}	69.4	−75.5	68.8	−63.8

Figure 3B. There is a strong temperature effect on both k_w^k and k_H^k, whose values are depicted in Table 2. The Arrhenius plot gives good straight lines in both cases. Using the standard Eyring equation, the activated parameters were determined from the gradient ($= -\Delta H^‡/R$) and the intercept ($= \ln(k/h) + \Delta S^‡/R$, with k being the Botlzmann' constant and h the Planck' constant) of the graph $\ln(k_i/T)$ against T^{-1} (with k_i being k_w or k_H, respectively to the processes water- or H^+-catalyzed, either for ketonization or enolization). The resulting values are gathered in Table 3.

General Base-Catalysis. The ketonization reaction was also studied in aqueous buffered solutions of acetic acid-acetate and of its chloro-derivatives at 25 °C and I = 0.25 M, controlled with NaCl. Parts A and B of Figure 4 show the observed rate constants as a function of both the buffer concentration and the pH of the solution for the case of acetic acid−acetate and chloroacetic acid−chloroacetate buffers, respectively. It can be seen that k_0 increases with both the [buffer] and the pH of the reaction medium. These features are typical characteristics of a general base-catalyzed reaction. At constant pH, k_0 increases linearly with total buffer concentration according to eq 8, where K_a represents the acidity constant of the acid form of the buffer.

$$k_0 = k_s + k_{buf}[AcO^-] = k_s + k_B \frac{K_a}{K_a + [H^+]}[buffer]_t \quad (8)$$

The values of the intercept at the origin (k_s) and the gradient, k_{buf} ($= k_B K_a/(K_a + [H^+])$) of k_o versus [buffer] plots obtained at constant pH, are collected in Table 4, along with values of k_s^k {$= k_s/(1 + K_E)$} and k_{buf}^k {$= k_{buf}/(1 + K_E)$}. One may observe that k_s ($= k_w + k_H[H^+]$) is practically pH-independent, but k_{buf} increases with pH, indicating that the basic form of the buffer catalyses the reaction, as it is assumed in eq 8. From the pK_a of the buffer and the measured pH, the acetate concentration, [AcO^-] (or the chloroacetate concentration, [$ClAcO^-$]) is determined at each buffer concentration. In that case, the plot of k_0, or k_0^k, against [AcO^-] (or [$ClAcO^-$]) should result in a straight line showing the same slope ($= k_B$ or k_B^k, respectively) independent of the pH of the experiment. The corresponding graphs are shown in parts C and D of Figure 4 for the case of k_0^k. The catalytic coefficients, k_B^k, obtained for each buffer are reported in Table 4. The Brönsted plot of $\log(k_B^k)$ against pK_a of the three acids studied led to a linear relationship, with a slope value equals to $\beta = 0.464 \pm 0.003$ ($r = 0.999_9$).

Discussion

Keto−Enol/Enolate Equilibria. The equilibria involved as in acid as in basic media in 2-acetylcyclohexanone was studied in the current work by UV-absorption spectroscopy, in a spectral region where the ketone exhibits negliglible absorption, since only the enolic species is available, the most straightforward measurement is of the rate of disappearance of the enol to form the equilibrium mixture. The obtained results indicate that ACHE is nearly 43% enolized in aqueous acid medium, $K_E = 0.72$. In alkaline medium, ACHE exists as the enolate ion: the overall pK_a was measured as 9.85, which together with the K_E value infers $pK_a^E = 9.47$ and $pK_a^K = 9.65$. These results agree, in part, with those of Riley and Long.[30] These authors studied the bromination of 2-acetylcyclohexanone in water at 0.10 M (NaCl) ionic strength by observing the decrease in absorbance at 390 nm due to bromine. By working with 4 × 10^{-3} M of ACHE, they determined the keto−enol equilibrium constant at 25 °C as $K_E = 0.41$, while the measured pH of an aqueous ACHE solution partially neutralized gives a

(30) Riley, T.; Long, F. A. *J. Am. Chem. Soc.* **1962**, *84*, 522.

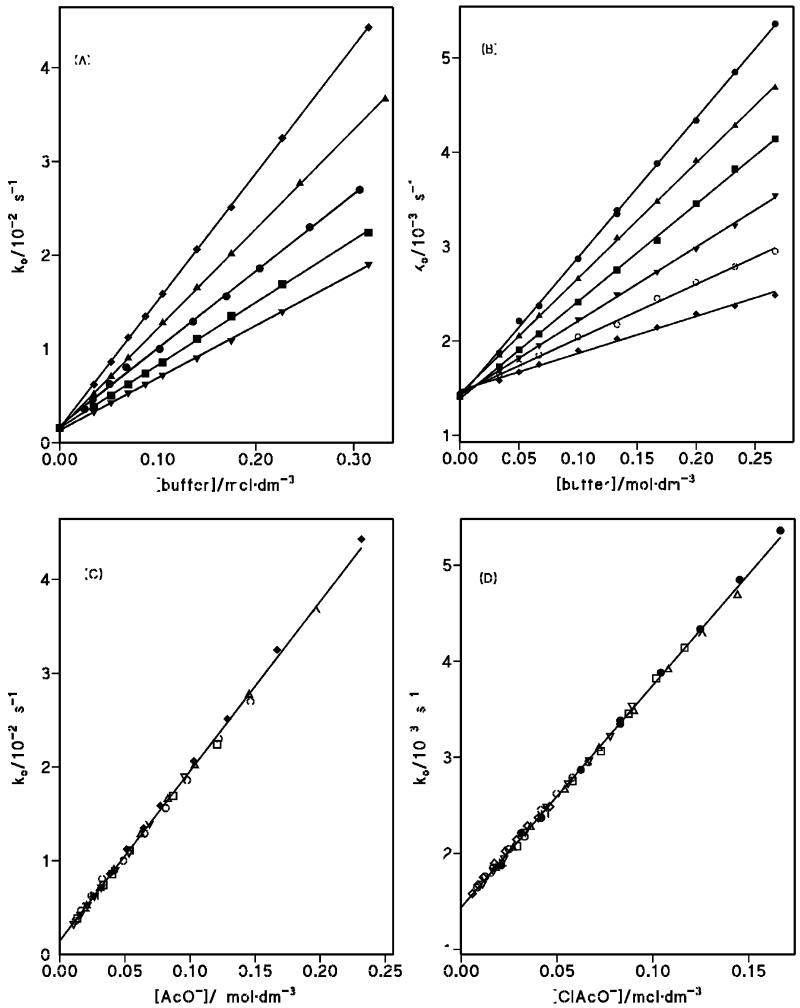

FIGURE 4. Variation of k_o for enol−ketonization as a function of (A) acetic acid-acetate buffer concentration and pH: (▼) 4.28, (■) 4.43, (●) 4.60, (▲) 4.85, and (◆) 5.08; and of (B) chloroacetic acid−chloroacetate buffer concentration and pH: (◆) 2.05, (○) 2.25, (▼) 2.43, (■) 2.62, (▲) 2.80, and (●) 2.95, at 25 °C and I = 0.25 M (NaCl). Values of k_o against (C) acetate ion concentration, pK_a = 4.64, and (D) chloroacetate ion concentration, pK_a = 2.73.

TABLE 4. First-Order, k_s, k_s^k, and Second-Order, k_{buf}, k_{buf}^k, Rate Constants Obtained in the Study of the Influence of Buffer Concentration in the Ketonization Reaction of ACHE at I = 0.25 M (NaCl) and 25 °C

pH	$k_s/10^{-3}$ s^{-1}	$k_{buf}/10^{-2}$[a]	$k_s^k/10^{-4}$ s^{-1}	$k_{buf}^k/10^{-2}$[a]	K_E	k_B (k_B^k)[a]	k_{HA}^k [a]
			Buffer of Acetic Acid−Acetate (pK_a = 4.64)[b]				
5.08	1.33 ± 0.07	13.61 ± 0.05	7.6	7.78	0.75	**0.179**[c]	**7.03 × 10^3**
4.81	1.36 ± 0.06	10.71 ± 0.02	7.7	6.08	0.76	**(0.104)**	
4.60	1.38 ± 0.06	8.46 ± 0.08	7.9	4.89	0.73		
4.43	1.39 ± 0.04	6.79 ± 0.04	8.1	3.66	0.73		
4.28	1.33 ± 0.05	5.38 ± 0.03	7.5	3.02	0.77		
			Buffer Chloroacetic Acid−Chloroacetate (pK_a = 2.73)[b]				
2.95	1.41 ± 0.02	1.475 ± 0.01	8.3	0.87	0.70	**0.0234**[c]	**7.03 × 10^4**
2.81	1.44 ± 0.02	1.222 ± 0.006	8.4	0.715	0.71	**(0.0134)**	
2.65	1.39 ± 0.01	1.030 ± 0.008	8.3	0.613	0.68		
2.43	1.43 ± 0.07	0.784 ±0.007	8.4	0.461	0.70		
2.25	1.45 ± 0.02	0.574 ± 0.010	8.6	0.340	0.69		
2.04	1.48 ± 0.01	0.392 ± 0.010	8.8	0.233	0.68		
			Buffer Dichloroacetic Acid−Dichloroacetate (pK_a = 1.35)[b]				
1.30	1.67 ± 0.02	0.248 ± 0.006	9.65	0.143	0.73	**5.26 × 10^{-3}**[c]	**4.03 × 10^5**
1.37	1.64 ± 0.01	0.270 ± 0.05	9.6	0.158	0.71	**(3.06 × 10^{-3})**	

[a] In mol^{-1} dm^3 s^{-1}. [b] From ref 36. [c] Determined from the slope of k_o (k_o^k) versus [base] plot; see Figure 4C,D.

pK_a value quite similar to that determined by us. We determined the keto−enol equilibrium constant of 2-acetylcyclopentanone as K_E = 0.40,[28] but cyclic compounds of six-membered rings have higher enol contents than the corresponding five-membered; therefore, the K_E = 0.72 determined in the present work appears to be more

reliable. The agreement between both pK_a values is expected, because both results are direct determinations; the different values obtained for K_E could be due to uncertainties in the end point (or to side reactions) in bromination titration as a consequence of the high enol content in ACHE; in fact, enolization is a H^+-catalyzed reaction contrarily to the reported results of Riley and Long[30] which are more proper for the situation where the bromination of the enol is the slow step.[24]

Mechanism of Keto−Enol Conversion. The conversion of the enol tautomer of a β-dicarbonyl compound to its keto isomer requires the removal of hydrogen from the carbonyl oxygen and placement of hydrogen on carbon. The reverse applies for the conversion of the keto into its enol isomer. The two processes are catalyzed by both acids and bases, which fact indicates that the hydrogens move as protons in the rate-determining step.

Acid-Catalyzed Keto−Enol Conversion. The reaction mechanism of enol ketonization involves rate-determining H^+-transfer from any available acid to the β-carbon atom of the enol or its enolate ion. Rate profiles shown in Figure 3 suggest β-carbon protonation of only the un-ionized enol by H^+. Therefore, in eq 7, k_w^k refers to the water assisted enol-ketonization reaction, whereas k_H^k is the rate constant H^+-catalyzed. Data in Table 2 show that k_w^k or k_H^k depend on the ionic strength. The former rate constant refers to a reaction between two polar molecules (enol + water), whereas the latter conforms to a reaction between an ion (H^+) and a polar molecule. At ionic strength higher than 0.1 M, the activity coefficients of nonelectrolytes are given by $\log \gamma_o = b_o I$, where b_o is an empirical constant.[31] For reactions between two nonelectrolytes (the case of k_w^k), or between an ion and a polar molecule (the case of k_H^k), the variation of γ_o with I implies that log k is a linear function of I. This is just the experimental observed behavior, with the following results: $\log(k_w^k) = (-3.073 \pm 0.004) - (0.098 \pm 0.008)I$ and $\log(k_H^k) = (-2.52 \pm 0.01) + (0.27 \pm 0.02)I$. The opposite effects of I on the two processes is a consequence of the different nature of the TS, vide infra, depending if the reaction is water- or H^+-catalyzed; thus, the slope of the linear plots log(k) versus I depends on the difference ($b_o^A + b_o^B - b_o^{\ddagger}$), where A and B refer to both reactants. The same effect is observed for the enolization process in agreement with the *principle of microscopic reversibility*.

Both processes are markedly affected by temperature. The activation parameters reported in Table 3 indicate that the keto−enol equilibrium of ACHE is not temperature dependent. This fact is easily understood if the standard enthalpies of formation of both isomers are considered, which can be estimated from bond-energies. The large and negative activation entropy values associated to the uncatalyzed process would be the expected ones for keto−enol interconversion involving a transition state that restricts the degree of freedom of *more than one water molecule* as postulated in Scheme 3.

Isotope Effects. At 25 °C, the values of the solvent isotope effects observed for the uncatalyzed reaction are $k_w^k(H_2O)/k_w^k(D_2O) = 8.2$, for enol−ketonization, and $k_w^e(H_2O)/k_w^e(D_2O) = 9.1$, for keto−enolization. Activation entropy values associated with the uncatalyzed process are in agreement with the solvent isotope effects determined for this reaction step.

SCHEME 3. Postulated Transition State for Keto−Enol Conversion in ACHE System

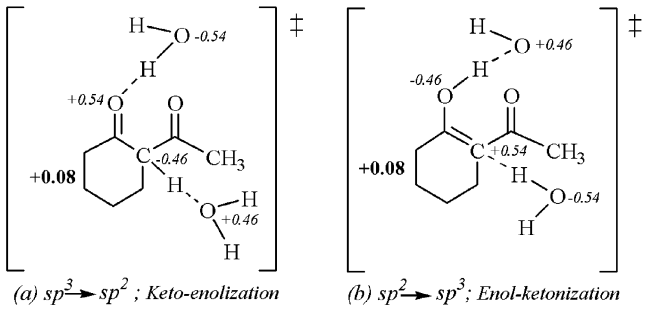

(a) $sp^3 \rightarrow sp^2$; Keto-enolization *(b) $sp^2 \rightarrow sp^3$; Enol-ketonization*

For an understanding of the previous figures, it is necessary to remember that when enol−ketonization goes on in D_2O solvent, the enol-H would be a deuteron (D) and its transfer would contribute an additional component to the isotope effect. Enol−ketonization involves proton/deuteron removal from oxygen by H_2O/D_2O, which, from chemical intuition one should to believe that this transfer—between two electronegative atoms-—should be fast, and the H/D transfer to carbon from H_2O/D_2O, whose process would expect to be rate-determining. Then as a O−H (D) bond is broken in the rate-determining step, a simple kinetic treatment of kinetic deuterium isotope effect in which the zero-point-energy difference between the stretching vibration of a O−H and O−D bond is allowed to disappear in the TS predicts $k(H_2O)/k(D_2O) = 10.6$ at 25 °C.[32] However, this theoretical maximum value, experimentally is found to be considerable lower. Variation of bending frequencies in TS affects the magnitude of isotope effects, and bending motions in general show much greater variation in frequency than do stretching motion. Since in enol-ketonization the C(2) changes from sp^2 to sp^3, then the hybridization of the activated complex is intermediate between them. But the bending vibration frequencies are lower in sp^2 than in sp^3 hybridization; thus, in enol−ketonization the bending vibration frequencies are higher for the TS than for the reactant. This fact decreases $k(H_2O)/k(D_2O)$ ratio (the maximum effect is 1.45).[33] In addition, the intramolecular H-bonds (O···H···O) in the enol may stabilize this isomer by >10 kcal/mol,[34] in other words, this effect increases the magnitude of $k(H_2O)/k(D_2O)$ ratio. By joining all these factors, the observed value of the isotope effect in enol−ketonization seems to be quite reasonable.

With regard to the H^+-catalyzed keto−enol transformation and proceeding now with keto−enolization, we assumed the reaction mechanism stated in Scheme 4. The preequilibrium protonation of the substrate by H_3O^+ leads to an increase in isotopically sensitive zero-point energy and an inverse solvent isotope effect on this step

(31) Brezonik, P. L. *Chemical Kinetics and Process Dynamics in Aquatic Systems*; Lewis Publishers: Florida, 1994; Chapter 3.

(32) Bell, R. P. *The Proton in Chemistry*; Chapman and Hall: London, 1973; Chapter 11.

(33) (a) Lorry, T. H.; Richardson, K. S. *Mechanism and Theory in Organic Chemistry*; Harper & Row: New York, 1987; Chapter 2. (b) Melander, L.; Saunders, W. H. *Reaction Rates of Isotopic Molecules*; John Wiley & Sons: New York, 1987; Chapter 6.

(34) (a) Jeffrey, G. A. *An Introduction to Hydrogen Bonding*; Oxford University Presss: New York, 1997. (b) Dziembowska, T.; Rozwadowski, Z. *Curr. Org. Chem.* **2001**, *5*, 289.

SCHEME 4. Reaction Mechanism of Acid-Catalyzed Enolization in ACHE System

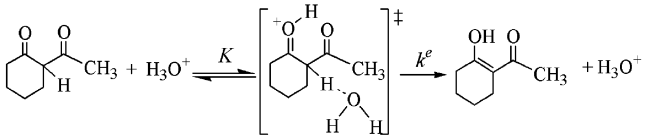

SCHEME 5. Reaction Mechanism of Base-Catalyzed Enol−Ketonization in ACHE System

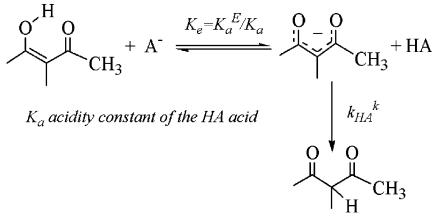

of $K(H_2O)/K(D_2O) = 0.6$ to 0.3.[35] This effect, however, is overwhelmed by the primary isotope effect produced in the rate-determining step, in which a C−H (D) bond is broken, and the net result is an overall isotope effect in the normal direction, but smaller: the experimental value is $k_H/k_D = 3.5$ (see Table 2).

Base-Catalyzed Keto−Enol Interconversion. In both ketonization and enolization processes, the general base catalysis is more pronounced than the proton-catalysis. The buffer catalytic coefficients, k_{buf} (or k_{buf}^k, k_{buf}^e) given in Table 4 can be separated into their general acid, k_{HA}, and general base, k_B, components (the latter increase with the strength of the base). Then eq 9 applies.

$$k_{buf} = k_B + (k_{HA} - k_B)\frac{[HA]}{[buffer]} \qquad (9)$$

The plot of k_{buf} (or k_{buf}^k or k_{buf}^e) against the fraction of the buffer present in the acid form, i.e., [HA]/[buffer], gives a good straight line with negative slope ($= k_{HA} - k_B$); the absolute value of the slope equals the intercept ($= k_B$), which means that only general base catalysis is occurring, i.e., k_{HA} is negligible. This general base catalysis observed in enol−ketonization indicates that the reaction is proceeding through base ionization of the enol in a rapid preequilibrium step followed by rate-determining carbon protonation of the enolate ion by the conjugate acid of the general base (Scheme 5). The rate law for this process can be rearranged to give an expression for the general acid catalytic coefficients of the enolate ion reaction, k_{HA}^k, in terms of K_a (the acidity constant of the conjugate acid) and K_a^E (the acidity constant determined for the enol) according to eq 10.

$$k_{HA}^k = \frac{K_a}{K_a^E} k_B^k \qquad (10)$$

The calculated k_{HA}^k values increase as expected with the strength of the acid as shown in Table 4. The Brönsted exponent obtained by least-squares analysis of the data gives $\alpha = 0.536 \pm 0.001$ in ketonization proton

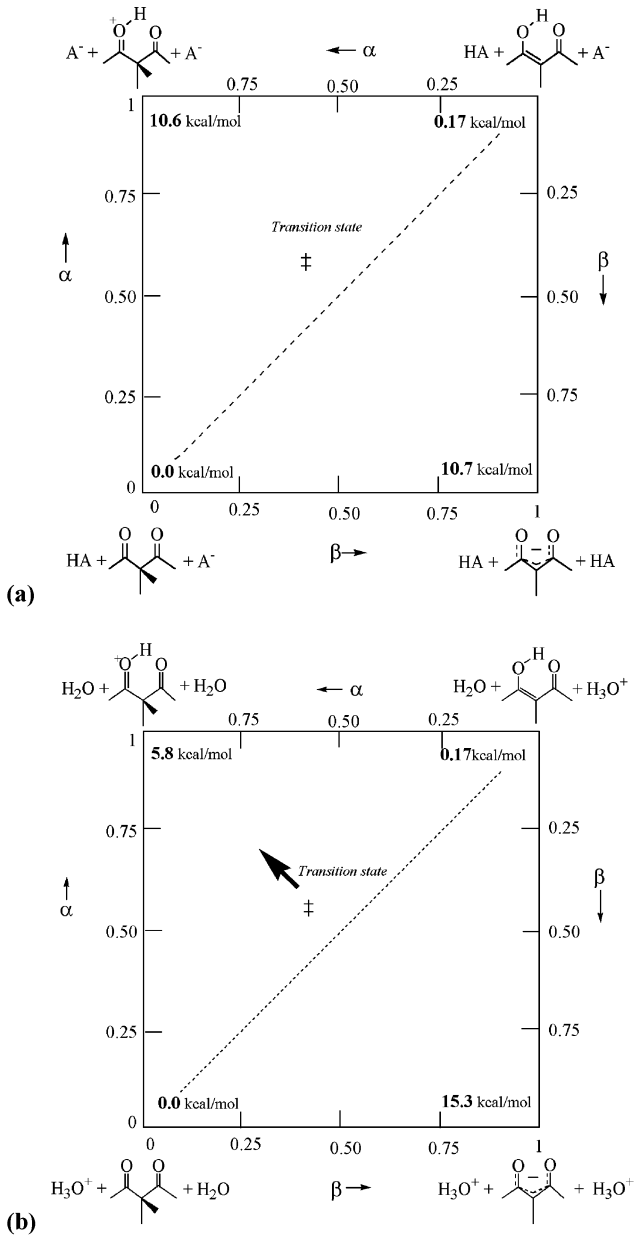

FIGURE 5. More O'Ferral−Jencks free-energy diagram for the (a) base-catalyzed and (b) acid-catalyzed keto−enol interconversion of 2-acetylcyclohexanone.

donation to carbon of enolate ion (this is equivalent to $\beta = 1 - \alpha = 0.464$ for proton removal from carbon in enolization).

This Brönsted exponent points to the formation of slightly unsymmetrical transition states. The *nature of the transition state* (TS) can be deduced as follow. The Brönsted exponents can be identified with extents of charge transfer at the TS. Then, by considering the enolization process, $\beta = 0.46$ means that a charge of +0.46 has been given to the *base* removing the hydrogen on carbon (e.g., a water molecule), which generates a negative charge of −0.46 on the ACHE molecule, and that a positive charge of +0.54 has been moved from the *acid* donating a hydrogen to the carbonyl oxygen, which generates +0.54 units of charge on the ACHE molecule and leaves a charge of −0.54 on the water molecule from

(35) Kresge, A. J. *Pure Appl. Chem.* **1964**, *8*, 243.
(36) Perrin, D. D. *pK$_a$ Prediction for Organic Acids and Bases*; Chapman and Hall: New York, 1981.

which this H^+ is being transferred (or +0.46 if the acid is H_3O^+). The net charge on the ACHE molecule is then −0.46 + 0.54 = +0.08. The Scheme 3 shows the overall transition state charge distribution. This result suggests that the keto−enol conversion is an overall base-catalyzed reaction with proton donation running ahead of proton removal. A transition state positively charged is reinforced by the general observation of that 1,3-dicarbonyl compounds form chelate complexes with metal cations, and, recently we postulated the existence of nitrosyl complex intermediate in the nitrosation of 1,1,1-trifluoro-3-(2-thenoyl)acetone,[25] of 2-acetylcyclopentanone,[28] and of the enol of 2-acetylcyclohexanone (see the following paper). On the other hand, a positively charged TS for keto−enol conversion will respond to structural changes in the same way as ester hydrolysis, as we have found in the study of the ester hydrolysis of ethyl-cyclohexanone-2-carboxylate.[26]

The More O'Ferrall−Jencks free-energy diagram suggested by the Brönsted coefficients in keto−enolization is given in Figure 5A, where the position of the transition state is indicated by the symbol ‡. The horizontal coordinate represents proton removal from carbon, with a scale equal to the Brönsted exponent β, and the vertical coordinate, with its scale equal to α, represents proton transfer to oxygen. The energies of various corners of this diagram can be calculated from the keto−enol equilibrium constant, $K_E = 0.72$, the acidity constant of the keto, $pK_a^K = 9.62$, the pK_a of the catalytic acid, and the pK_a^{KH} of the keto isomer protonated on the oxygen. This latter species undoubtedly is a strong acid with $pK_a^{KH} < -5$; e.g., the numbers shown on the diagram are for a catalytic acid of $pK_a = 1.75$ (the midpoint of our Brönsted correlation) and a pK_a^{KH} of the protonated enol equal to −6. When the catalyst system is replaced by H_3O^+ ($pK_a = -1.74$) and H_2O, the corresponding energies are those indicated in Figure 5B. It may be seen that the free-energies of the reactant and product corners have not changed, but those of the other two corners, enolate and protonated-keto at oxygen, have higher and lower energy values, respectively. These changes will shift the *transition state* in the direction shown by the arrow, away from the enolate ion and toward the protonated keto. This means that, the reaction mechanism of H^+-catalyzed ketonization resembles more to a consecutive mechanism with preequilibrium protonation of the substrate, in total accordance with the observed isotope effects (vide supra).

Conclusions

In alkaline medium, 2-acetylcyclohexanone undergoes rapid ionization to give the enolate. The overall pK_a was measured as 9.85. When the alkaline solution is made acidic, the enol tautomer is rapidly recovered with a yield of 100%. But, subsequently, the 2-acetylcyclohexanone enol ketonizes slowly in aqueous acid medium until to reach a 43% enol content at equilibrium. Both ketonization and enolization are acid and general-base catalyzed reactions. The base catalysis is stronger than the acid catalysis and increases with the strength of the base. The isotopic effect, along with the Brönsted exponents, determined independently for each reaction, points to a reaction mechanism in which a proton-transfer occurs in the rate-determining step. The More O'Ferrall−Jencks free-energy diagrams constructed from Brönsted exponents suggest a slightly unsymmetrical transition states bearing a net positive charge.

Acknowledgment. Financial support from the Dirección General de Investigación (Ministerio de Ciencia y Tecnología) of Spain (Project No. BQU2000-0239-C02) is gratefully acknowledged.

JO026629X